Vibrational Frequencies and Spectroscopic Constants for 1 $^3A'$ HNC and 1 $^3A'$ HOC^+ from High-Accuracy Quartic Force Fields

Ryan C. Fortenberry,[*,†,§] T. Daniel Crawford,[‡] and Timothy J. Lee[*,¶]

Georgia Southern University, Department of Chemistry, Statesboro, GA 30460 U.S.A., Virginia Tech, Department of Chemistry, Blacksburg, Virginia 24061, U.S.A., and NASA Ames Research Center, Moffett Field, California 94035-1000, U.S.A.

E-mail: rfortenberry@georgiasouthern.edu; Timothy.J.Lee@nasa.gov

[*]To whom correspondence should be addressed
[†]Georgia Southern University
[‡]Virginia Tech
[¶]NASA Ames Research Center
[§]Previous address: NASA Ames Research Center Moffett Field, California 94035-1000, U.S.A.

Abstract

The spectroscopic constants and vibrational frequencies for the 1 $^3A'$ states of HNC, DNC, HOC^+, and DOC^+ are computed and discussed in this work. The reliable CcCR quartic force field based on high-level coupled cluster *ab initio* quantum chemical computations is exclusively utilized to provide the anharmonic potential. Then, second-order vibrational perturbation theory and vibrational configuration interaction methods are employed to treat the nuclear Schrödinger equation. Second-order perturbation theory is also employed to provide spectroscopic data for all molecules examined. The relationship between these molecules and the corresponding 1 $^3A'$ HCN and HCO^+ isomers is further developed here. These data are applicable to laboratory studies involving formation of HNC and HOC^+ as well as astronomical observations of chemically active astrophysical environments.

Keywords: Astrochemistry; Quartic Force Fields; Coupled Cluster Theory; Vibrational Perturbation Theory; Vibrational Configuration Interaction Theory; Vibrational Frequencies; Triplet States

Introduction

The presence of HNC and the isoelectronic HOC^+ has been known in the interstellar medium (ISM) for some time.[1–5] HNC has been hypothesized as a product in the dissociative recombination of interstellar[6] $HCNH^+$ in molecular clouds[7,8] as one possible astronomical synthetic pathway. High-resolution experimental studies have recently examined the vibrational frequencies of HNC and the deuterated isotopologue, DNC.[9–11] Additionally, highly-excited vibrational lines of HNC were observed toward the carbon-rich star IRC +10 216 with the Herschel Space Observatory[12] before the space-based telescope closed its eyes in the spring of 2013.

There has been speculation that the lowest energy triplet states of HCN, HNC, HCO^+, and HOC^+ contribute to rotational signals observed in the THz spectral range of labora-

tory studies designed to simulate various astronomical environments.[13–16] Previous CASPT2 computations report a 4.47 eV 1 $^3A' \leftarrow \tilde{X}^1\Sigma^+$ excitation energy for HNC (Ref. 17), which is similar in energy for the same excitation in HCN at 4.69 eV (CASPT2/ANO-L from Ref. 18). Additionally, the energy separation between 1 $^3A'$ HCN and 1 $^3A'$ HNC has been computed to be 10.9 kcal/mol [CCSD(T)/aug-cc-pVTZ] and even less between 1 $^3A'$ HCO^+ and 1 $^3A'$ HOC^+ at 2.5 kcal/mol.[19] As a result, overlap in the rotational signals for the two isomers of the respective nitrogen- or oxygen-containing species generated is likely. Resolution of their individual spectra would benefit from reference data in order to distinguish the spectral features.

Quartic force field (QFF) computations of vibrational frequencies and spectroscopic constants for the $\tilde{X}$ $^1\Sigma^+$ states of both HNC and HOC^+ have long served as examples of the accuracy that quantum chemical calculations can provide.[20,21] Building from that framework and the two decades of development since then,[22–26] the largely unexamined vibrational frequencies and spectroscopic constants for the 1 $^3A'$ states of HNC and HOC^+ are investigated here, whereas earlier rovibrational studies have produced reference data for the 1 $^3A'$ states of HCN and HCO^+.[19] Additionally, with continuing growth in infrared (IR) and far IR telescopic capability, reference data for these molecules could assist in the chemical characterization of astronomical spectra taken with instruments on plane- or space-based telescopes such as the Stratospheric Observatory For Infrared Astronomy (SOFIA) and the upcoming James Webb Space Telescope (JWST), as well as the ground-based Atacama Large Millimeter Array (ALMA).

Computational Details

The procedure for the computation of the vibrational frequencies and spectroscopic constants of 1 $^3A'$ HNC and HOC^+ closely mirrors that used for the study of the 1 $^3A'$ states of HCN and HCO^+ (Ref. 19) and used in the study of other systems.[22,23,27–29] Due to the open-

shell nature of these triplet systems, restricted open-shell reference wavefunctions[30–32] are combined with the coupled cluster singles, doubles, and perturbative triples [CCSD(T)] level of theory.[33] The geometries are optimized with Dunning's correlation consistent aug-cc-pV5Z basis set[34–36] refined by corrections for core-correlation from the Martin-Taylor (MT) basis sets designed to properly treat inclusion of the core orbitals in the CCSD(T) computations.[37] From these reference geometries, central difference displacements of 0.005 Å for the bond lengths and 0.005 radians for the bond angles are generated from the simple-internal coordinates leading to a grid composed of 129 points. Since this is a fourth-order Taylor series approximation to the anharmonic potential function, the displacements are treated up to fourth-order to give the QFF. At each point on the QFF surface, a three-point complete basis set (CBS) limit extrapolation[38] energy is computed from utilization of Dunning's augmented triple, quadruple, and quintuple zeta basis sets. To this CBS energy, corrections for core-correlation and scalar relativity[39] with the cc-pVTZ-DK basis set are included to form the CcCR (CBS + core-Correlation + Relativistic) QFF. All electronic structure computations employ the MOLPRO 2010.1 quantum chemistry package.[40]

The equilibrium geometry and the force constants are produced from a least-squares fitting of the points in the QFF where the sum of squared residuals is on the order of 10^{-17} a.u.^{2}. Cartesian derivatives are subsequently determined using the INTDER program,[41] and fed into the SPECTRO program[42] where vibrational second-order perturbation theory[43–45] returns the spectroscopic constants and vibrational frequencies. Different from the second-order vibrational perturbation theory (VPT2) results, the vibrational configuration interaction (VCI) frequencies are produced from the MULTIMODE program[46,47] after the QFFs are transformed into a Morse-cosine coordinate system.[25,48]

Results and Discussion

Geometrical Data and Spectroscopic Constants

The difference in CCSD(T)/aug-cc-pV5Z energy for the optimized geometries of the $\tilde{X}\ ^1\Sigma^+$ state and the $1\ ^3A'$ state of HNC gives an adiabatic excitation energy of 4.64 eV, similar to the 4.47 eV transition energy computed previously with CASPT2.[17] This is a $\pi \rightarrow \pi^*$ excitation out of the highest energy π bonding orbital in linear HNC into the lowest energy π antibonding orbital. As such, a (core)$3a'^2 4a'^2 5a'^2 1a''^2 6a'^1 7a'^1$ configuration is produced in the bent triplet from the (core)$3\sigma^2 4\sigma^2 5\sigma^2 1\pi^4 2\pi^0$ orbital configuration present in the linear singlet. The same process occurs in the HCN isomer, as well, with a similar CCSD(T)/aug-cc-pV5Z adiabatic excitation energy of 4.84 eV.[19] Previous adiabatic computations have placed the energy difference between the $1\ ^3A'$ states of HCN and HNC between 10.4 and 10.9 kcal/mol.[19] Here, we refine this non-zero-point value to 10.3 kcal/mol from the more complete CcCR energies of both triplet isomers.

The $1\ ^3A'$ HNC equilibrium geometry fit from the CcCR QFF given in Table 1 is in line with that produced from previous CASPT2 computations[17] but differs enough to show the refinement brought about by the higher-order computations employed here. The dipole moments have a larger variance between the two methods, 1.06 D from CCSD(T)/aug-cc-pV5Z computations based on the CcCR geometry and 1.2963 D from the CASPT2 computation and geometry, but they differ by as much as one would expect between second-order perturbation theory and coupled cluster quantum chemical methods. For comparison, a previous CCSD(T)/aug-cc-pVTZ optimized geometry dipole moment of $1\ ^3A'$ HNC is 1.05 D.[19] When analyzed with respect to the CcCR $1\ ^3A'$ HCN structure, HNC has an understandably different geometry, especially for the bond angle which decreases from 120.587° for ∠H−C−N to 112.151° for ∠H−N−C. Zero-point (R_α) vibrational averaging for the HNC geometry increases each of the bond lengths as well as the bond angle as compared to the HNC equilibrium geometry. The B- and C-type rotational constants are subsequently decreased upon

vibrational averaging whereas the A-type constant increases from 624.286 4 GHz to 626.373 7 GHz when the vibrational effects are included.

Since HOC^+ is isoelectronic to HNC, the 1 $^3A'$ state results from the same excitation scheme as that given above. The CCSD(T)/aug-cc-pV5Z adiabatic 1 $^3A' \leftarrow \tilde{X}\ ^1\Sigma^+$ excitation energy for HOC^+ is 4.21 eV. This is substantially less than the 5.86 eV adiabatic excitation energy for HCO^+ computed in the same manner.[19] The CcCR energy difference between the 1 $^3A'$ states of HOC^+ and HCO^+ is a mere 1.4 kcal/mol, 0.2 kcal/mol less than CCSD(T)/aug-cc-pV5Z computations at the optimized CCSD(T)/aug-cc-pVTZ geometries previously indicated.[19] However, the barriers to isomerization computed previously[19] indicate that rearrangement of the isomers has a significant energy cost at more than 40 kcal/mol for both HCO^+/HOC^+ and HCN/HNC.

The 1.80 D dipole moment for 1 $^3A'$ HOC^+ (also given in Table 1) is smaller than the corresponding HCO^+ isomer at 2.51 D but nearly coincident with the CCSD(T)/aug-cc-pVTZ 1.81 D dipole computed as part of our earlier study.[19] The B- and C-type rotational constants (whether from equilibrium or vibrationally averaged) for 1 $^3A'$ HNC and HOC^+ are equivalent between the molecules to within 0.5 GHz. However, the A-type constants should allow for them to be spectrally distinguished. Deuteration of either molecule studied here noticeably changes the rotational constants, as one would expect.

The symmetry-internal quadratic, cubic, and quartic force constants are given in Table 2. The gradients are zero by construction. The force constants given in Table 2 are numbered sequentially from the geometrical parameters given in Table 1 where coordinate 1 corresponds to the X−C bond, coordinate 2 corresponds to the X−H bond, and coordinate 3 corresponds to ∠H−X−C with X = N or O. Table 3 contains the other spectroscopic constants including the vibration-rotation interaction constants, the quartic and sextic centrifugal distortion constants, and the Watson S-reduced Hamiltonian terms for both 1 $^3A'$ HNC and HOC^+ as well as their respective deuterated isotopologues.

Vibrational Frequencies

The fundamental harmonic and anharmonic vibrational frequencies as well as the first overtones and combination bands of 1 $^3A'$ HNC, DNC, HOC^+, and DOC^+ are listed in Table 4. The VPT2 1 $^3A'$ HNC and HOC^+ computations require input of a $2\nu_2 = \nu_1$ Fermi resonance. VPT2 for both DNC and DOC^+ requires input of a $\nu_3 + \nu_2 = \nu_1$ Fermi resonance. No Coriolis or Darling-Dennison resonances are present in these systems. The MULTIMODE VCI computations are complete and exact at the three mode representation (3MR) level since all fundamental vibrational modes for these non-linear triatomic molecules can be coupled at this level. Basis set convergence is defined here as a change of less than 1.0 cm^{-1} with an increase in more than 100 basis functions. Convergence is achieved for each of the molecules in this study upon the inclusion of 420 basis functions in the computation. The bond stretching bases are each composed of 36 Gaussian integration points, 31 primitive harmonic oscillator basis functions, and 20 Hermite-Gauss (HEG) quadrature points. The bending bases contain 26 Gaussian integration points, 23 primitive harmonic oscillator bases, and 14 HEG points. These basis setups are of the same size or larger as those employed to study larger tetraatomics where the hydrogen stretching frequencies, for instance, have been computed to be within 5 cm^{-1} or even better than 1 cm^{-1} as compared to gas phase experiment.[23,49,50] The CcCR QFF is the only QFF used in this study since previous work has shown this QFF to be the most cost-effective means of computing highly-accurate rovibrational reference data.[19,22,23,27,28]

The CcCR 1 $^3A'$ HNC harmonic frequencies from Table 4 highlight the difference in geometry brought about from isomerization originating with 1 $^3A'$ HCN. N−H stretches occur at higher frequencies relative to C−H stretches, and such is highlighted here. Even the C−N bond stretch varies between the isomers decreasing from 1589.5 cm^{-1} in 1 $^3A'$ HCN to 1568.9 cm^{-1} in 1 $^3A'$ HNC. Previous CASPT2 computations[17] for 1 $^3A'$ HNC report a lower harmonic frequency N−H stretch at 3103 cm^{-1} relative to the CcCR 3189.3 cm^{-1} harmonic frequency. The ν_2 and ν_3 modes have higher harmonic frequencies in the previous

work[17] compared to the CcCR QFF.

The VPT2 and VCI anharmonic frequencies should be more accurate than either of the sets of harmonic frequencies reported. The ν_1 fundamental and the combination bands and overtones containing it are the most anharmonic of the frequencies by magnitude. VPT2 and VCI treat the nuclear Schrödinger equation through different means, but they arrive at similar if not identical frequencies for 1 $^3A'$ HNC when using the CcCR QFF. The N−C ν_2 stretch is computed to be 1534.0 cm^{-1} for both methods. Further consistency is present in the hydride stretch where VPT2 reports this mode to be 2939.9 cm^{-1} while VCI is exactly 1.0 cm^{-1} less. The bending mode has a larger difference between the two methods, but it is still only 2.2 cm^{-1}. Larger variances between the methods begin to arise in the overtones and combination bands. This is epitomized in the $\nu_1 + \nu_2$ combination band. VPT2 reports a 4456.2 cm^{-1} frequency while VCI reports this frequency to be 4447.1 cm^{-1}. However, this 9.1 cm^{-1} difference is fairly small since combination bands are more difficult to model with QFFs than the fundamentals. Regardless, the consistency in the methods indicates a marked measure of reliability for these frequencies.

1 $^3A'$ DNC continues the consistency reported for the standard isotopologue. Within the Born-Oppenheimer approximation used in the formulation of the QFF, the force constants are the same between 1 $^3A'$ HNC and DNC. VPT2 and VCI consider the different effects of the heavier atom in solving the nuclear problem. As such, each of the fundamental vibrational frequencies for DNC are less than their corresponding HNC frequencies. The ν_2 stretching frequency is identical between VPT2 and VCI even though it is 8.5 cm^{-1} lower in frequency at 1523.5 cm^{-1} after deuteration. The ν_1 and ν_3 modes are actually more consistent between VPT2 and VCI for DNC than they are for HNC. Additionally, VPT2 and VCI are in much better agreement for the overtones and combination bands of DNC, as well. The largest difference between the methods is 5.2 cm^{-1}, again for the $\nu_1 + \nu_2$ combination band, but $2\nu_1$, $2\nu_2$, and $\nu_2 + \nu_3$ have VPT2-VCI differences of 1.5 cm^{-1} or less.

The ν_1 O−H stretch of 1 $^3A'$ HOC$^+$ is the highest frequency mode of all the fundamentals

reported in this set of triplet triatomics. It is 3146.6 cm^{-1} from CcCR VPT2 and 3146.0 cm^{-1} from CcCR VCI, a further indication that the frequencies are well described with either method. The ν_2 O−H stretch differs by 0.1 cm^{-1} here, and the ν_3 bending frequency differs by 1.6 cm^{-1} with VCI producing a 1166.8 cm^{-1} frequency for this mode. Again, the CcCR QFF is providing consistent results with either vibrational calculation method. The $2\nu_1$ and $2\nu_2$ overtones are quite consistent between the methods as they were for DNC. The largest VPT2-VCI difference for HOC^+ for any of the fundamentals, overtones, or combination bands is the $2\nu_3$ bending overtone. VPT2 gives 2306.1 cm^{-1} while VCI is 2299.5 cm^{-1}, a difference of 6.6 cm^{-1}.

Deuteration of 1 $^3A'$ HOC^+ to yield 1 $^3A'$ DOC^+ also reduces the vibrational frequencies as compared to the standard isotopologue. All of the VPT2 fundamental frequencies, however, are within 1.0 cm^{-1} of their VCI counterparts. The $\nu_1+\nu_3$ combination band represents the largest VPT2-VCI discrepancy with the frequencies differing between the two methods by 6.3 cm^{-1}. However, the ν_2 fundamental and $2\nu_2$ overtone are computed to possess nearly the same frequencies wether VPT2 or VCI is employed.

Conclusions

Since the $\tilde{X}$ $^1\Sigma^+$ forms of HNC and HOC^+ are known to exist in the ISM, and it is reasonable to believe that the 1 $^3A'$ forms of HNC and HOC^+ can arise in various interstellar environments, an understanding of their vibrational and rotational properties would serve to better inform astronomical observations and laboratory studies where they may be found. The corresponding isomers of each (i.e., HCN and HCO^+) have been examined previously,[19] and this study represents a completion of the rovibrational analysis for minima on each of the respective potential energy surfaces. The 1 $^3A'$ HCN and HCO^+ isomers are shown here with highly-accurate methods to be only 10.3 kcal/mol and 1.4 kcal/mol, respectively, lower in energy than the corresponding HNC and HOC^+ isomers, though it was shown previously

that there is a large barrier (> 40 kcal/mol) separating the respective minima. Thus, if triplet HNC or HOC^+ are formed, they will not easily isomerize to the lower energy HCN or HCO^+ isomer. Indeed, there has already been speculation that the lowest triplet states of HCN, HNC, HCO^+, and HOC^+ might be present in laboratory experiments designed to simulate astrophysical conditions. The $1\ ^3A' \leftarrow \tilde{X}\ ^1\Sigma^+$ HNC excitation is 4.64 eV and lower at 4.21 eV for HOC^+. However, if $1\ ^3A'$ HNC and HOC^+ (as well as HCN and HCO^+) result from a formation mechanism favoring triplet states in astronomical regions where the molecular density and collisional probability are low, then they could exist for a long time lacking a radiative mechanism to the ground electronic singlet state.

The fundamental vibrational frequencies for both $1\ ^3A'$ HNC and HOC^+, as well as the deuterated isotopologues are reported in this study. The set of frequencies for each molecule are in very good agreement between the VPT2 and VCI methods with both making use of the CcCR QFF. Additionally, the overtones and combination bands are also fairly consistent giving a strong indication that the computed results presented here are reliable. The spectroscopic constants provided from second-order perturbation theory also give the potential for further insights into the behavior of these molecules. All could be of benefit for analysis of spectra whether taken in the laboratory or from an astronomical observation.

Acknowledgement

The NASA Postdoctoral Program administered by Oak Ridge Associated Universities through a contract with NASA as well as funds provided by Georgia Southern University financially supported the work done by RCF. The National Science Foundation (NSF) Multi-User Chemistry Research Instrumentation and Facility (CRIF:MU) award CHE-0741927 provided the necessary computer hardware employed in this work. TDC and RCF gratefully acknowledge this support. Additionally, TDC received NSF award CHE-1058420 and is thankful for this support. TJL was funded by NASA Grant 10-APRA10-0167. TJL and RCF also acknowledge support from NASA's Laboratory Astrophysics 'Carbon in the Galaxy' Con-

sortium Grant (NNH10ZDA001N). Creation of the figures employed the CheMVP program developed at the University of Georgia's Center for Computational Quantum Chemistry.

References

(1) Woods, R. C.; Gudeman, C. S.; Dickman, R. L.; Goldsmith, P. F.; Huguenin, G. R.; Irvine, W. M.; Hjalmarson, A.; Nyman, L.-A.; Olofsson, H. The HCO^+/HOC^+ abundance ratio in molecular clouds. *Astrophys. J.* **1983**, *270*, 583–588.

(2) Ziurys, L. M.; Apponi, A. J. Confirmation of Interstellar HOC^+: Reevaluating the $[HCO^+]/[HOC^+]$ Abundance Ratio. *Astrophys. J. Lett.* **1995**, *455*, L73–L76.

(3) Snyder, L. E.; Buhl, D. Detection of Several New Interstellar Molecules. *Annals of the New York Academy of Sciences* **1972**, *194*, 17–24.

(4) Blackman, G. L.; Brown, R. D.; Godfrey, P. D.; Gunn, H. I. The microwave spectrum of HNC: Identification of U90.7. *Nature* **1976**, *261*, 395–396.

(5) Zuckerman, B.; Morris, M.; Palmer, P.; Turner, B. E. Observations of CS, HCN, U89.2, and U90.7 in NGC 2264. *Astrophys. J.* **1972**, *173*, L125–L129.

(6) Ziurys, L. M.; Turner, B. E. $HCNH^+$: A new interstellar molecular ion. *Astrophys. J.* **1986**, *302*, L31–L36.

(7) Allen, T. L.; Goddard, J. D.; Schaefer III, H. F. A Possible Role for Triplet H_2NC^+ Isomers in the Formation of HCN and HNC in Interstellar Clouds. *J. Chem. Phys.* **1980**, *73*, 3255–3263.

(8) DeFrees, D. J.; Binkley, J. S.; Frisch, M. J.; McLean, A. D. Is N-Protonated Hydrogen Isocyanide, H_2NC^+, an Observable Interstellar Species. *J. Chem. Phys.* **1986**, *85*, 5194–5199.

(9) Mellau, G. C. The ν_1 band system of HNC. *J. Molec. Spectrosc.* **2010**, *264*, 2–9.

(10) Mellau, G. C. Complete experimental rovibrational eigenenergies of HNC up to 3743 cm^{-1} above the ground state. *J. Chem. Phys.* **2010**, *133*, 164303.

(11) Amano, T. Submillimeter-wave rotational spectra of DNC in highly excited vibrational states observed in an extended negative glow discharge. *J. Molec. Spectrosc.* **2011**, *267*, 158–162.

(12) Daniel, F.; Agundez, M.; Cernicharo, J.; DeBeck, E.; Lombaert, R.; Decin, L.; Kahane, C.; Guèlin, M.; Müller, H. S. P. Herschel/HIFI observation of highly excited rotational lines of HNC toward IRC +10 216. *Astron. Astrophys.* **2012**, *542*, A37.

(13) Botschwina, P.; Horna, M.; Matuschewskia, M.; Schick, E.; Sebaldb, P. Hydrogen Cyanide: Theory and Experiment. *J. Molec. Struct.* **1997**, *400*, 119–137.

(14) Drouin, B. J.; Yu, S.; Miller, C. E.; Müller, H. S.; Lewen, F.; Brünken, S.; Habara, H. Terahertz spectroscopy of oxygen, O_2, in its $^3\Sigma_g^-$ and $^1\Delta$ electronic states THz Spectroscopy of O_2. *J. Quant. Spectrosc. Rad. Trans.* **2010**, *111*, 1167–1173.

(15) Drouin, B. J.; Yu, S.; Pearson, J. C.; Gupta, H. Terahertz spectroscopy for space applications: 2.5-2.7 THz spectra of HD, H_2O and NH_3. *J. Molec. Struct.* **2011**, *1006*, 2–12.

(16) Hu, X.; Xie, C.; Xie, D.; Guo, H. State-to-state quantum dynamics of the $N(^4S)$ + $CH(X\ ^2\Pi) \rightarrow CN\ (X\ ^2\Sigma^+, A\ ^2\Pi)$. *J. Chem. Phys.* **2013**, *139*, 124313.

(17) Pd, R.; Chandra, P. Ground and excited states of HNC, NH, and NH_2 transients: *Ab initio* geometries, electronic structures, and molecular properties. *J. Chem. Phys.* **2001**, *117*, 7450–7460.

(18) Li, J.; Wang, Y.; Jiang, B.; Ma, J.; Dawes, R.; Xie, D.; Bowman, J. M.; Guo, H. Communication: A chemically accurate global potential energy surface for the HO + $CO \rightarrow H + CO_2$ reaction. *J. Chem. Phys.* **2012**, *136*, 041103.

(19) Fortenberry, R. C.; Huang, X.; Crawford, T. D.; Lee, T. J. The 1 $^3A'$ HCN and 1 $^3A'$ HCO^+ Vibrational Frequencies and Spectroscopic Constants from Quartic Force Fields. *J. Phys. Chem. A.* **2013**, 9324–9330.

(20) Lee, T. J.; Dateo, C. E.; Gazdy, B.; Bowman, J. M. Accurate Quartic Force Fields and Vibrational Frequencies for HCN and HNC. *J. Phys. Chem.* **1993**, *97*, 8937–8943.

(21) Martin, J. M. L.; Taylor, P. R.; Lee, T. J. Accurate *ab initio* quartic force fields for the ions HCO^+ and HOC^+. *J. Chem. Phys.* **1993**, *99*, 286–292.

(22) Huang, X.; Lee, T. J. A procedure for computing accurate ab initio quartic force fields: Application to HO_2^+ and H_2O. *J. Chem. Phys.* **2008**, *129*, 044312.

(23) Fortenberry, R. C.; Huang, X.; Francisco, J. S.; Crawford, T. D.; Lee, T. J. The *trans*-HOCO radical: fundamental vibrational frequencies, quartic force fields, and spectroscopic constants. *J. Chem. Phys.* **2011**, *135*, 134301.

(24) Fortenberry, R. C.; Huang, X.; Crawford, T. D.; Lee, T. J. High-Accuracy Quartic Force Field Calculations for the Spectroscopic Constants and Vibrational Frequencies of $1^1A'$ *l*-C_3H^-: A Possible Link to Lines Observed in the Horsehead Nebula PDR. *Astrophys. J.* **2013**, *772*, 39.

(25) Fortenberry, R. C.; Huang, X.; Yachmenev, A.; Thiel, W.; Lee, T. J. On the Use of Quartic Force Fields in Variational Calculations. *Chem. Phys. Lett.* **2013**, *574*, 1–12.

(26) Fortenberry, R. C.; Huang, X.; Schwenke, D. W.; Lee, T. J. Limited rotational and rovibrational line lists computed with highly accurate quartic force fields and *ab initio* dipole surfaces. *Spectrochim. Acta, Part A.* **2013**, *in press*.

(27) Huang, X.; Lee, T. J. Accurate *ab initio* quartic force fields for NH and CCH and rovibrational spectroscopic constants for their isotopologs. *J. Chem. Phys.* **2009**, *131*, 104301.

(28) Huang, X.; Taylor, P. R.; Lee, T. J. Highly accurate quartic force field, vibrational frequencies, and spectroscopic constants for cyclic and linear $C_3H_3^+$. *J. Phys. Chem. A* **2011**, *115*, 5005–5016.

(29) Fortenberry, R. C.; Huang, X.; Francisco, J. S.; Crawford, T. D.; Lee, T. J. Vibrational frequencies and spectroscopic constants from quartic force fields for cis-HOCO: The radical and the anion. *J. Chem. Phys.* **2011**, *135*, 214303.

(30) Gauss, J.; Lauderdale, W. J.; Stanton, J. F.; Watts, J. D.; Bartlett, R. J. Analytic energy gradients for open-shell coupled-cluster singles and doubles (CCSD) calculations using restricted open-shell HartreeâĂŤFock (ROHF) reference functions. *Chem. Phys. Lett.* **1991**, *182*, 207–215.

(31) Lauderdale, W. J.; Stanton, J. F.; Gauss, J.; Watts, J. D.; Bartlett, R. J. Many-body perturbation theory with a restricted open-shell HartreeâĂŤFock reference. *Chem. Phys. Lett.* **1991**, *187*, 21–28.

(32) Watts, J. D.; Gauss, J.; Bartlett, R. J. CoupledâĂŘcluster methods with noniterative triple excitations for restricted open-shell Hartree-Fock and other general single determinant reference functions. Energies and analytical gradients. *J. Chem. Phys.* **1993**, *98*, 8718–8733.

(33) Raghavachari, K.; Trucks., G. W.; Pople, J. A.; Head-Gordon, M. A fifth-order perturbation comparison of electron correlation theories. *Chem. Phys. Lett.* **1989**, *157*, 479–483.

(34) Dunning, T. H. Gaussian basis sets for use in correlated molecular calculations. I. The atoms boron through neon and hydrogen. *J. Chem. Phys.* **1989**, *90*, 1007–1023.

(35) Peterson, K. A.; Dunning, T. H. Benchmark calculations with correlated molecular wave functions. VII. Binding energy and structure of the HF dimer. *J. Chem. Phys.* **1995**, *102*, 2032–2041.

(36) Kendall, R. A.; Dunning, T. H.; Harrison, R. J. Electron affinities of the firstâĂŘrow atoms revisited. Systematic basis sets and wave functions. *J. Chem. Phys.* **1992**, *96*, 6796–6806.

(37) Martin, J. M. L.; Taylor, P. R. Basis set convergence for geometry and harmonic frequencies. Are h functions enough? *Chem. Phys. Lett.* **1994**, *225*, 473–479.

(38) Martin, J. M. L.; Lee, T. J. The atomization energy and proton affinity of NH_3. An *ab initio* calibration study. *Chem. Phys. Lett.* **1996**, *258*, 136–143.

(39) Douglas, M.; Kroll, N. Quantum electrodynamical corrections to the fine structure of helium. *Ann. Phys.* **1974**, *82*, 89–155.

(40) Werner, H.-J. et al. MOLPRO, version 2010.1, a package of ab initio programs. 2010; see http://www.molpro.net.

(41) Allen, W. D.; coworkers, 2005; $INTDER$ 2005 is a general program written by W. D. Allen and coworkers, which performs vibrational analysis and higher-order non-linear transformations.

(42) Gaw, J. F.; Willets, A.; Green, W. H.; Handy, N. C. In *Advances in Molecular Vibrations and Collision Dynamics*; Bowman, J. M., Ratner, M. A., Eds.; JAI Press, Inc.: Greenwich, Connecticut, 1991; pp 170–185.

(43) Mills, I. M. In *Molecular Spectroscopy - Modern Research*; Rao, K. N., Mathews, C. W., Eds.; Academic Press: New York, 1972; pp 115–140.

(44) Watson, J. K. G. In *Vibrational Spectra and Structure*; During, J. R., Ed.; Elsevier: Amsterdam, 1977; pp 1–89.

(45) Papousek, D.; Aliev, M. R. *Molecular Vibration-Rotation Spectra*; Elsevier: Amsterdam, 1982.

(46) Carter, S.; Bowman, J. M.; Handy, N. C. Extensions and tests of "multimodes": A code to obtain accurate vibration/rotation energies of many-mode molecules. *Theor. Chem. Acc.* **1998**, *100*, 191–198.

(47) Bowman, J. M.; Carter, S.; Huang, X. MULTIMODE: a code to calculate rovibrational energies of polyatomic molecules. *Int. Rev. Phys. Chem.* **2003**, *22*, 533–549.

(48) Dateo, C. E.; Lee, T. J.; Schwenke, D. W. An accurate quartic force-field and vibrational frequencies for HNO and DNO. *J. Chem. Phys.* **1994**, *101*, 5853–5859.

(49) Fortenberry, R. C.; Huang, X.; Francisco, J. S.; Crawford, T. D.; Lee, T. J. Quartic force field predictions of the fundamental vibrational frequencies and spectroscopic constants of the cations $HOCO^+$ and $DOCO^+$. *J. Chem. Phys.* **2012**, *136*, 234309.

(50) Huang, X.; Fortenberry, R. C.; Lee, T. J. Protonated nitrous oxide, $NNOH^+$: Fundamental vibrational frequencies and spectroscopic constants from quartic force fields. *J. Chem. Phys.* **2013**, *139*, 084313.

Figure 1: The CcCR equilibrium geometry of 1 $^3A'$ HNC.

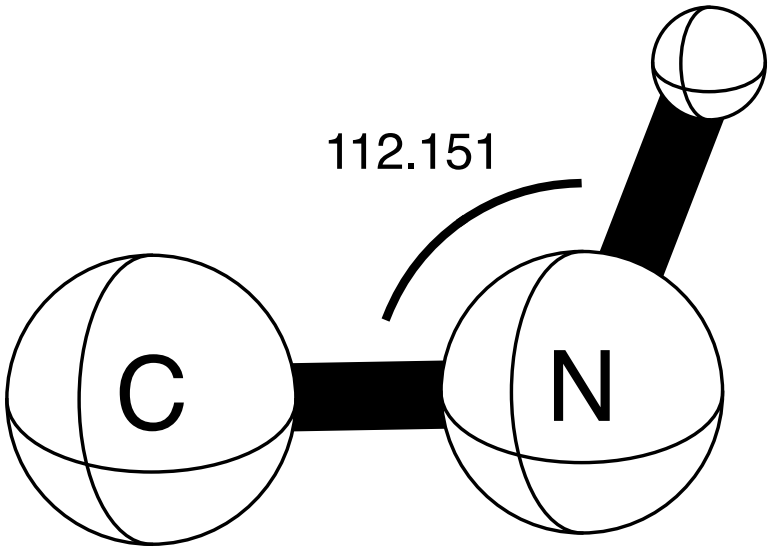

Figure 2: The CcCR equilibrium geometry of 1 $^3A'$ HOC^+.

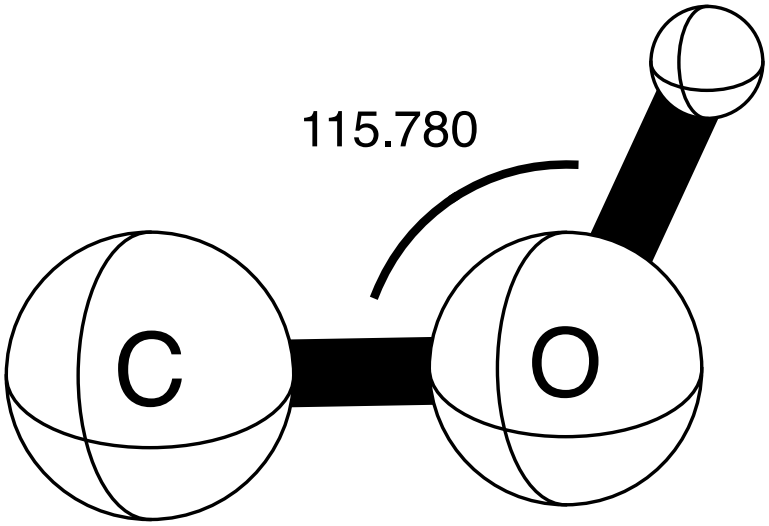

Table 1: The CcCR QFF 1 $^3A'$ HNC and 1 $^3A'$ HOC$^+$ Minimum Energy Structures (in Å and degrees) and Rotational Constants (in GHz).

		Equilibrium		Zero-Point	
Molecule		This work	Previous[a]	Standard	Deuterated
1 $^3A'$ HNC	R(N−C)	1.261 56	1.2709	1.265 80	1.266 15
	R(N−H)	1.032 80	1.0417	1.049 00	1.045 17
	∠H−N−C	112.151	111.63	112.325	112.235
	$A_{e/0}$	624.286 4		626.373 7	356.142 0
	$B_{e/0}$	44.809 22		44.696 35	40.840 85
	$C_{e/0}$	41.805 09		41.504 93	36.419 59
	μ	1.06	1.2963		
1 $^3A'$ HOC$^+$	R(O−C)	1.224 90		1.229 27	1.229 50
	R(O−H)	0.993 92		1.008 66	1.005 15
	∠H−O−C	115.780		116.119	115.959
	$A_{e/0}$	708.961 6		717.653 0	404.429 5
	$B_{e/0}$	44.945 07		44.782 93	41.085 23
	$C_{e/0}$	42.262 07		41.943 11	37.077 49
	μ	1.80			

[a] 10/(8,2) CASPT2 computations from Rajendra and Chandra (Ref. 17).

Table 2: The CcCR QFF Quadratic, Cubic, and Quartic Force Constants (in mdyn/Å^n·rad^m) for the simple-internal coordinates of 1 $^3A'$ HNC and HOC$^+$.

HNC				HOC$^+$			
F_{11}	9.641 120	F_{1111}	369.16	F_{11}	11.387 673	F_{1111}	431.05
F_{21}	0.383 265	F_{2111}	22.85	F_{21}	0.331 626	F_{2111}	19.34
F_{22}	5.656 329	F_{2211}	-16.99	F_{22}	6.360 166	F_{2211}	-10.40
F_{31}	0.638 345	F_{2221}	12.26	F_{31}	0.705 791	F_{2221}	5.41
F_{32}	0.144 040	F_{2222}	218.31	F_{32}	0.081 788	F_{2222}	286.31
F_{33}	0.751 132	F_{3111}	-6.78	F_{33}	0.758 736	F_{3111}	-1.53
F_{111}	-69.3948	F_{3211}	-0.69	F_{111}	-82.3006	F_{3211}	-0.64
F_{211}	-3.4084	F_{3221}	0.60	F_{211}	-3.2506	F_{3221}	0.82
F_{221}	2.9664	F_{3222}	-2.03	F_{221}	1.6407	F_{3222}	-1.17
F_{222}	-42.4825	F_{3311}	-2.35	F_{222}	-47.3035	F_{3311}	2.92
F_{311}	-2.9653	F_{3321}	-0.75	F_{311}	-1.4453	F_{3321}	-0.82
F_{321}	-0.2343	F_{3322}	0.47	F_{321}	-0.2912	F_{3322}	0.65
F_{322}	-0.3804	F_{3331}	0.58	F_{322}	-0.3408	F_{3331}	0.37
F_{331}	-0.6733	F_{3332}	0.50	F_{331}	-0.6832	F_{3332}	1.37
F_{332}	0.0139	F_{3333}	-0.61	F_{332}	-0.1290	F_{3333}	-1.29
F_{333}	-0.7522			F_{333}	-1.0334		

Table 3: The CcCR Vibration-Rotation Interaction Constants, Quartic and Sextic Centrifugal Distortion Constants, and S Reduced Hamiltonian Terms for 1 $^3A'$ HNC and HOC$^+$.

	Vib-Rot Constants (MHz)				Distortion Constants				Watson S Reduction			
	mode	α^A	α^B	α^C	(MHz)			(Hz)	(MHz)			(Hz)
HNC	1	31523.1	-115.7	20.0	τ'_{aaaa}	-1080.703	10^{-3} Φ_{aaa}	509.210	D_J	0.139	H_J	-0.174
	2	2944.3	519.5	433.7	τ'_{bbbb}	-0.652	Φ_{bbb}	0.056	D_{JK}	5.695	H_{JK}	57.640
	3	-38642.0	-191.0	159.6	τ'_{cccc}	-0.494	Φ_{ccc}	-0.124	D_K	264.342	10^{-3} H_{KJ}	5.567
					τ'_{aabb}	-21.472	10^{-3} Φ_{aab}	15.462	d_1	-0.010	10^{-3} H_K	503.586
					τ'_{aacc}	-2.372	Φ_{abb}	103.723	d_2	-0.002	h_1	0.025
					τ'_{bbcc}	-0.555	10^{-3} Φ_{aac}	-9.854			h_2	0.070
							Φ_{bbc}	-0.417			h_3	0.020
							Φ_{acc}	5.539				
							Φ_{bcc}	-0.214				
							Φ_{abc}	120.024				
DNC	1	12493.5	13.2	120.0	τ'_{aaaa}	-407.104	10^{-3} Φ_{aaa}	122.646	D_J	0.113	H_J	-0.054
	2	1587.0	446.8	368.8	τ'_{bbbb}	-0.610	Φ_{bbb}	0.534	D_{JK}	2.561	H_{JK}	41.101
	3	-17726.9	-195.0	134.1	τ'_{cccc}	-0.352	Φ_{ccc}	-0.008	D_K	99.102	10^{-3} H_{KJ}	60.494
					τ'_{aabb}	-10.855	10^{-3} Φ_{aab}	4.293	d_1	-0.016	10^{-3} H_K	122.545
					τ'_{aacc}	-0.223	Φ_{abb}	71.536	d_2	-0.004	h_1	0.089
					τ'_{bbcc}	-0.435	10^{-3} Φ_{aac}	-4.208			h_2	0.159
							Φ_{bbc}	-0.578			h_3	0.047
							Φ_{acc}	8.667				
							Φ_{bcc}	-0.078				
							Φ_{abc}	91.369				
HOC$^+$	1	31610.2	-11.5	82.8	τ'_{aaaa}	-1601.803	10^{-6} Φ_{aaa}	1.007	D_J	0.127	H_J	-0.082
	2	6108.6	457.5	403.1	τ'_{bbbb}	-0.584	Φ_{bbb}	0.109	D_{JK}	6.140	H_{JK}	20.640
	3	-55101.4	-135.0	165.2	τ'_{cccc}	-0.460	Φ_{ccc}	-0.086	D_K	394.189	10^{-3} H_{KJ}	8.999
					τ'_{aabb}	-22.260	10^{-3} Φ_{aab}	21.388	d_1	-0.008	10^{-3} H_K	997.663
					τ'_{aacc}	-3.278	Φ_{abb}	73.068	d_2	-0.002	h_1	0.034
					τ'_{bbcc}	-0.507	10^{-3} Φ_{aac}	-12.422			h_2	0.047
							Φ_{bbc}	-0.241			h_3	0.015
							Φ_{acc}	-4.631				
							Φ_{bcc}	-0.112				
							Φ_{abc}	96.065				
DOC$^+$	1	12393.9	82.5	153.0	τ'_{aaaa}	-585.740	10^{-3} Φ_{aaa}	228.978	D_J	0.103	H_J	0.031
	2	3840.9	386.4	343.7	τ'_{bbbb}	-0.543	Φ_{bbb}	0.484	D_{JK}	2.728	H_{JK}	13.591
	3	-25342.2	-134.4	147.4	τ'_{cccc}	-0.331	Φ_{ccc}	0.014	D_K	143.603	H_{KJ}	650.885
					τ'_{aabb}	-11.150	10^{-3} Φ_{aab}	6.076	d_1	-0.013	10^{-3} H_K	228.313
					τ'_{aacc}	-0.533	Φ_{abb}	47.679	d_2	-0.003	h_1	0.081
					τ'_{bbcc}	-0.397	10^{-3} Φ_{aac}	-5.458			h_2	0.109
							Φ_{bbc}	-0.374			h_3	0.037
							Φ_{acc}	4.279				
							Φ_{bcc}	0.012				
							Φ_{abc}	77.466				

Table 4: The CcCR QFF harmonic and anharmonic (from VPT and VCI) fundamental vibrational frequencies (in cm^{-1}) for 1 $^3A'$ HCN, HCO^+, and their respective deuterated forms.

Molecule	Description	Mode	Harmonic	Previous[a]	VPT	VCI
HNC	a' N−H stretch	ν_1	3189.3	3103	2923.9[b]	2922.9
	a' N−C stretch	ν_2	1568.9	1578	1534.0	1534.0
	a' H−N−C bend	ν_3	1165.7	1200	1137.1	1134.9
		$2\nu_1$	6378.6		5591.4	5592.9
		$2\nu_2$	3137.8		3037.3	3038.4
		$2\nu_3$	2331.4		2253.7	2245.0
		$\nu_1+\nu_2$	4758.2		4456.2	4447.1
		$\nu_1+\nu_3$	4355.0		4050.2	4044.8
		$\nu_2+\nu_3$	2734.6		2666.5	2664.3
DNC	a' N−D stretch	ν_1	2329.4		2183.5[c]	2184.8
	a' N−C stretch	ν_2	1555.4		1523.5	1523.5
	a' D−N−C bend	ν_3	891.5		875.0	874.1
		$2\nu_1$	4658.8		4232.0	4232.3
		$2\nu_2$	3110.9		3017.7	3017.3
		$2\nu_3$	1783.0		1739.1	1735.6
		$\nu_1+\nu_2$	3884.9		3710.0	3705.8
		$\nu_1+\nu_3$	3220.9		3055.2	3051.7
		$\nu_2+\nu_3$	2446.9		2395.9	2394.4
HOC^+	a' O−H stretch	ν_1	3370.7		3146.6[b]	3146.0
	a' O−C stretch	ν_2	1661.9		1630.1	1630.2
	a' H−O−C bend	ν_3	1208.3		1168.4	1166.8
		$2\nu_1$	6741.4		6080.4	6080.4
		$2\nu_2$	3323.8		3230.1	3230.6
		$2\nu_3$	2416.6		2306.1	2299.5
		$\nu_1+\nu_2$	5032.6		4774.1	4770.6
		$\nu_1+\nu_3$	4579.0		4297.4	4292.5
		$\nu_2+\nu_3$	2870.2		2798.4	2797.4
DOC^+	a' O−D stretch	ν_1	2456.1		2333.7[c]	2334.3
	a' O−C stretch	ν_2	1643.9		1612.8	1612.9
	a' D−O−C bend	ν_3	922.7		900.9	900.1
		$2\nu_1$	4912.1		4559.5	4557.1
		$2\nu_2$	3287.7		3194.8	3194.8
		$2\nu_3$	1845.4		1784.2	1780.9
		$\nu_1+\nu_2$	4099.9		3948.5	3943.4
		$\nu_1+\nu_3$	3378.8		3228.4	3222.1
		$\nu_2+\nu_3$	2566.6		2517.5	2516.3

[a]Harmonic 10/(8,2) CASPT2 frequencies from Rajendra and Chandra (Ref. 17).
[b]These modes are affected by a $2\nu_2 = \nu_1$ Fermi Resonance.
[c]These modes are affected by a $\nu_3 + \nu_2 = \nu_1$ Fermi Resonance.